npj | heritage science

Article

https://doi.org/10.1038/s40494-025-02080-4

# Multiple analytical characterization of Madao chariot horse crests from a Chu noble tomb

Check for updates

Lulu Li[1,3], Yingchun Fu[1,3] ✉, Yaoyao Zhang[1], Jianye Liu[2] & Shuya Wei[1] ✉

Madao is a kind of chariot horse crest comprising tassels wound on sticks mounted to oval wooden bases affixed to the foreheads of horses. To reveal complex materials and techniques of Madao artifacts, the study employs a range of approaches including polarized light microscopy, SEM-EDS, XRD, and THM-Py-GC/MS. The results indicated that wooden oval bases were composed of a ground layer and a lacquer layer. Microscopic analysis confirmed that the crushed and size-sorted clay particles were identified as unheated natural clays serving as inorganic fillers in the ground layer. The lacquer coated on the wooden base was urushiol-based lacquer without drying oils modified. Besides, tassels were also characterized by consisting of *Hydrophasianus chirurgus* feathers secured with bast fibers. These results demonstrate how Chu artisans engineered composite materials to meet the specific performance requirements of horse components.

The Warring States Period (475–221BCE) marked the first apex of lacquer development in ancient China, with Chu state as technological epicenter[1]. Research of Chu lacquer objects reveals the pinnacle of technological and artistic sophistication achieved in ancient China. Extensive excavations of Chu tombs, such as Wuwangdun[2] and Jiuliandun[3], have unearthed a large quantity of lacquerwares. These include sacrificial vessels, weapons, routine utensils, musical instruments, and chariot and horse components, offering a valuable insight into the daily lives of the elite in that era. The manufacturing techniques of armours[4], bian qing (a type of ancient Chinese musical instrument)[5], ear cups and boxes[1] have been revealed by scientific approaches, primarily focusing on weapons, sacrificial vessels, routine utensils and musical instruments. In contrast, the materials and techniques of chariot and horse components have received less relative attention.

During the Warring States Period, strict regulations governed the hierarchical classification of carriages and horses for the purpose of noble travel in ancient China. The Madao (马纛), a chariot horse crest affixed to the horse's forehead, signaled high rank. Archaeological evidence confirms its early Warring States origin[6], with it evolving into an exclusive ornament for imperial chariot horses during the Qin (221–206 BCE) and Han (202 BCE–220 CE) dynasties[7]. Its standardized form featured a tassel-wrapped stick affixed to a lacquered wooden oval base (Fig. 2a). From the technical perspective, the Madao was manufactured by multiple materials, forming a distinctive type of composite lacquerwares. Aesthetically, it achieved a subtle balance between the flowing tassels and stable base, making it an exemplary representation of kinetic art among ancient chariot and horse components. Research on Madao can provide insights into the manufacturing process and technical details of chariot and horse components in the early China, and help to understand the significance of early Chinese rituals. Between September 2013 and January 2015, archaeological excavations at the Wangshanqiao No.1 tomb (abbreviated as Wangshanqiao M1) in Wangshan Village, Jingzhou City, Hubei Province (see Fig. 1), unearthed a number of Madao artifacts. This site is a typical tomb of the high nobility of the Chu State, belonging to "*Zhongjiuyin*" (中厩尹), a grandson of the king of Chu State[8]. Given the widespread deterioration of Madao artifacts[6], the structurally intact specimens from Wangshanqiao M1 offer exceptional research materials.

The current scientific and technological analysis of lacquerwares is predominantly oriented towards the examination of lacquering materials and techniques. The microscope is utilized to observe the number of layers, color, and thickness of the lacquer film, which is one of the most beneficial means to study lacquering structure[9]. Scanning electron microscopy equipped with energy-dispersive spectroscopy (SEM-EDS), X-ray diffraction (XRD), and Raman spectroscopy are commonly used to reveal the pigments and inorganic fillers in lacquer film[10]. Pyrolysis gas chromatography-mass spectrometry (Py-GC/MS) offers significant advantages, including high sensitivity, the ability to avoid the necessity for sample pretreatment, and minimal sample consumption, making it ideal for analyzing organic components in cultural relics. The technique of pyrolysis-gas chromatography-mass spectrometry with thermally assisted hydrolysis and methylation (THM-Py-GC/MS) has emerged as a leading analytical

[1]Institute of Cultural Heritage and History of Science & Technology, Key Laboratory of Archaeomaterials and Conservation, Ministry of Education, University of Science and Technology Beijing, Beijing, China. [2]Jingzhou Museum, Hubei, China. [3]These authors contributed equally: Lulu Li, Yingchun Fu.
✉e-mail: ycfu@ustb.edu.cn; sywei66@hotmail.com

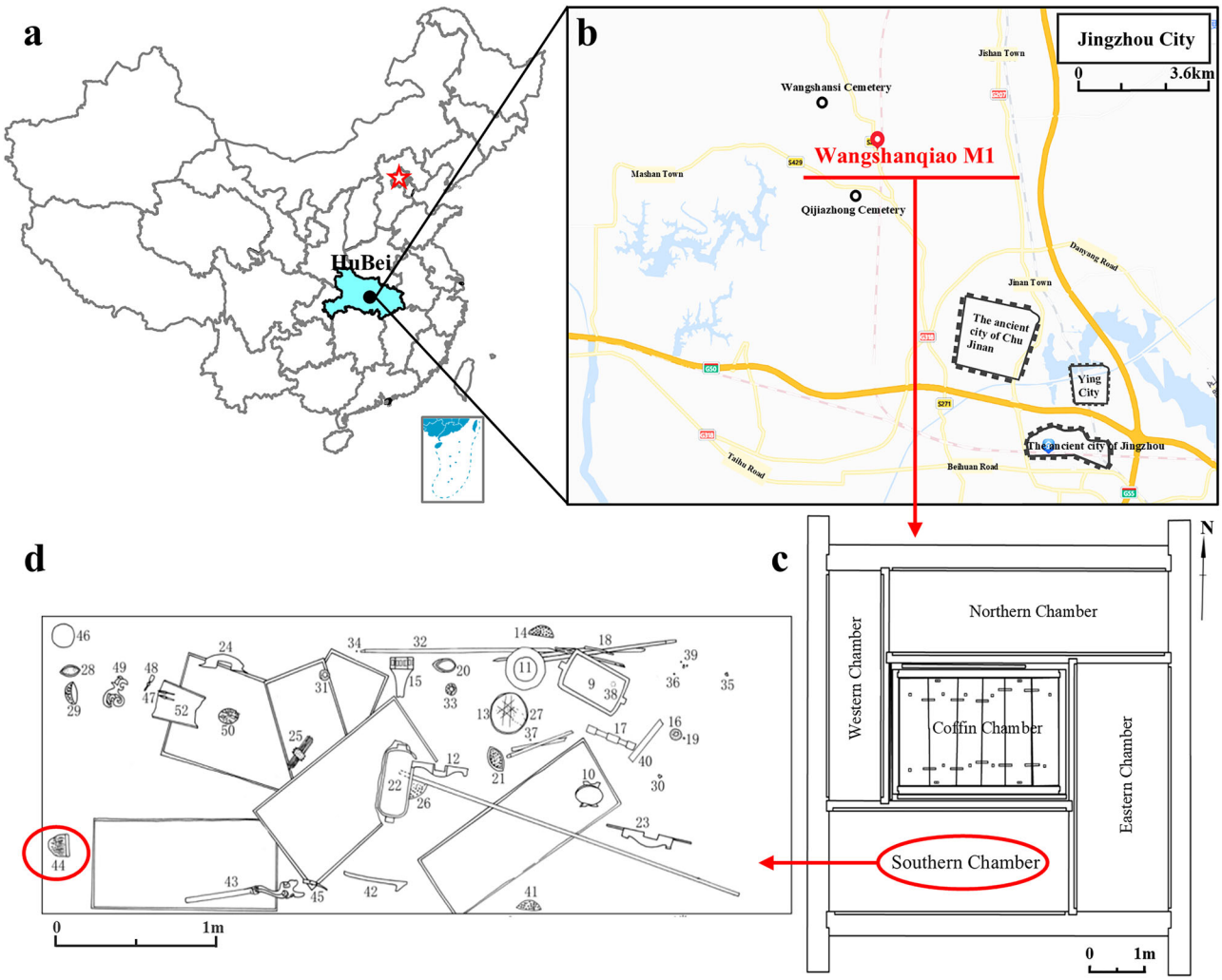


**Fig. 1 | Sample provenance and excavation location of Wangshanqiao M1.** **a** Location of Wangshanqiao M1 in Hubei Province (China). Black point: Wangshanqiao M1. Red pentagram: National capital (Beijing). **b** Location of Wangshanqiao M1 in Jingzhou City. Red horizontal line: Excavation site of Wangshanqiao M1. Grey outline: The ancient city of Chu Jinan Scale, Ying City, The ancient city of Jinzhou. Black circle: Qijiazhong Cemtery, Wangsahnsi Cemetery. **c** Schematic plan of the outer coffin chamber in Wangshanqiao M1. Red circle: Southern Chamber. **d** Schematic diagram of funerary objects distribution in the southern chamber. Red circle: M1:N44 sample.

method[11]. This technique has been found to be particularly effective in analyzing of Asian lacquers, providing comprehensive compositional insights into catechol-rich saps from the three main species of trees belonging to the Anacardiaceae family used in Asian lacquers, as well as a wide range of lacquer additives[12]. Additionally, Py-GC/MS facilitates rapid and accurate fiber compositional analysis, a particularly valuable process when dealing with micro-samples in heritage conservation[13,14]. Py-GC/MS enables preliminary differentiation between plant and animal fibers based on molecular composition, effectively narrowing down the identification scope. Although micro-morphological observation remains the mainstream method for fiber analysis, Py-GC/MS provides crucial corroborative evidence from a chemical perspective. The combination of these two techniques offers mutual complementation and verification, leading to precise identification of the tassel fiber type.

In order to elucidate the manufacturing paradigm of Madao artifacts, a comprehensive analysis was performed on the Madaos excavated from Wangshanqiao M1. The analytical protocol was initiated with optical microscopy for observing photographs of the cross-section of lacquer films and fiber morphology. Subsequent complementary SEM-EDS and XRD analyses were conducted to determine the elemental composition and crystalline phases of the inorganic constituents. Concurrently, the particulate morphologies were evaluated through SEM imaging to detect any evidence of thermal processing. The organic materials of the lacquer film and tassels were ultimately characterized using Py-GC/MS techniques.

## Methods

### Samples of Madao from the Chu tomb

Humid burial conditions caused severe degradation of Madao tassel and stick components. The outlooking of the excavated twenty-six Madaos are similar, with black lacquer on the surface. According to the request of archaeologists, M1:N44 Madao was selected as the representative specimen due to its exceptional state of preservation and complete retention of constituent materials. The M1:N44 Madao was excavated in the southern chamber of Wangshanqiao M1. In order to obtain the most comprehensive information possible about the archaeological Madao, a variety of locations were sampled, the details of which are shown in Fig. 2. The lacquer film sample in Fig. 2f was taken from a raised area on the surface of the base where the wooden substrate was exposed, ensuring structural integrity. The sample was divided equally into two portions. The one was mounted in epoxy resin for microstructure analysis, SEM-EDS, and XRD. The other was used for THM-Py-GC/MS analysis. The fiber samples in Fig. 2d and e were collected from the top of the wooden rod. Cross-sectional examination revealed the presence of two distinct fiber colors. Each type was sampled separately for polarized light micro analysis and Py-GC/MS (Fig. 8).

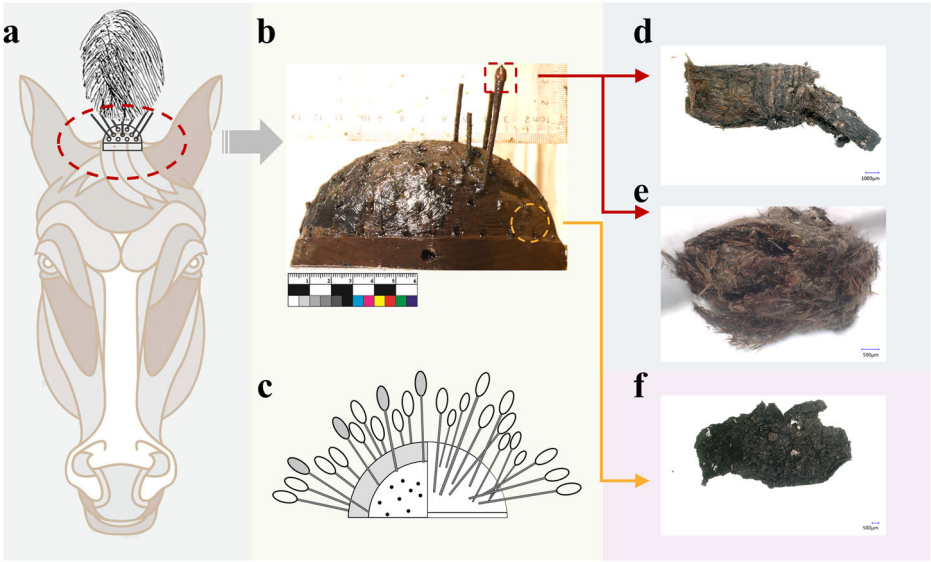


**Fig. 2 | Schematic diagram of M1:N44 Madao with samples. a** Schematic of Madao's position on the horse's forehead (red dotted circle). **b** The photo of M1:N44 Madao. Red dotted rectangle: Sampling location of the fiber samples. Yellow dotted circle: Sampling location of the lacquer film sample. **c** Sectional drawing of M1:N44 Madao. **d** Side view of fiber samples. **e** Cross-section view of fiber samples. **f** Front view of lacquer film sample.

### Optical microscope

The cross-section images of the samples were obtained by means of the VHX-6000 ultra-depth-of-field three-dimensional video microscope (Keyence, Japan) and the BX53 optical microscope (Olympus, Japan).

### Scanning electron microscopy with energy dispersive spectrometry (SEM-EDS)

A proportion of the sample fragments was mounted in epoxy resin and then polished with metallographic sandpaper of various grades, namely #600, #1000, #1500, #2000, #2500 and lapping pastes of size of 0.5 μm. Finally, the sample was coated with gold.

The elemental composition of the samples was characterized using a LEO-1450 (Zeiss, Germany) equipped with a NORAN 7 EDS (Thermo Scientific, America). An acceleration voltage of 20 kV was applied.

### X-ray diffraction (XRD)

XRD analysis was performed using a diffractometer (D8 Discover, Bruker) equipped with Cu Kα radiation from a source operated at 50 kV and 1000 μA. The scanning range of 2θ was from 20.0° to 80.0° with stepwise acquisition (6 steps), where each 12.0° increment required a dwell time of 30 s, yielding an effective scanning rate of 0.4°/min. The analysis of XRD data was conducted utilizing the ICDD PDF-2 database.

### Polarizing optical microscope

The fibers were agent employed was a Herzberg stain (iodine-zinc chloride, purchased from Beijing Lunghua Science and Technology extracted from the samples, dispersed, and a small quantity was placed on dry, clean slides with forceps for staining. The staining Co).

### Thermal assisted hydrolysis and methylation pyrolysis coupled with gas chromatography/mass spectrometry (THM-Py-GC/MS)

The pyrolysis-gas chromatography/mass spectrometry measurements were carried out using a pyrolyzer PY-3030D (Frontier Lab, Japan) attached to a gas chromatograph and mass spectrometry GC/MS-QP2010Utra (Shimadzu, Japan).

A capillary column Ultra Alloy-5 (MS/ HT) with a 0.25 mm internal diameter, 0.25 μm film thickness and 30 m length (Frontier Lab, Japan) was chosen in order to provide an adequate separation of the components. The pyrolysis process was conducted at 600 °C, with the pyrolyzer interface was set at 300 °C and the injector at 280 °C. The initial temperature of the oven was set at 50 °C with a gradient of 10 °C per min to 280 °C, which was held for 20 min. The carrier gas was helium with an inlet pressure of 100 kPa and a split ratio of 1:100. The electronic pressure control was set to the constant flow mode. Ions were generated by electron ionization (70 eV) within the ionization chamber of the mass spectrometer. The mass spectrometer was scanned from $m/z$ 50 to 750 with a cycle time of 0.5 s.

The procedure for thermal assisted hydrolysis and methylation pyrolysis (THM-Py-GC/MS) with TMAH analysis was performed as follows: ~0.1 mg of the samples were placed in a sample cup, and then 3 μL of 25% aqueous TMAH solution (Sinopharm Chemical Reagent Co., Ltd, China) were added with a micro syringe to the sample. The cup was introduced into the pyrolyzer (furnace) by the autosampler and pyrolyzed immediately, afterwards the temperature program of the GC/MS was initiated.

## Results

### Microstructure and elemental analysis of the lacquer film

The lacquering materials and techniques of the Madao's lacquered base comprise two principal components.

Firstly, microstructure and elemental analysis of the lacquer film revealed the following key findings. The morphology of the cross-section of the black lacquer sample from the Madao's lacquered base (Fig. 2f) was analyzed using bright field (BF) optical microscopy with halogen lamp illumination and SEM. As demonstrated in Fig. 3, the lacquer film is composed of two layers, namely a black lacquer layer on the surface (12~14 μm, L1 in Fig. 3) and a ground layer beneath (42 μm, L2 in Fig. 3). A sparse distribution of inorganic particles is observable within the ground layer. The lacquered wooden base of the Madao is notable for its absence of painted decoration, consisting exclusively of lacquer and ground layers. This configuration corresponds to the monochrome lacquering technique that is characteristic of black lacquerware[15].

EDS analyses revealed distinct inorganic compositional features across the lacquer layers. The results of the study are presented in Table 1. The analysis of all layers revealed a predominant presence of carbon and oxygen from organic components. Despite the absence of identifiable inorganic particles in the L1 lacquer layer as determined by backscattered electron (BSE) imaging, elemental mapping of A-1 area revealed an obvious concentrations of Si (2.6 wt%), Ca (10.2 wt%), and Fe (12.2 wt%). A-1 area was in direct contact with the burial soil. Given that Fe and Ca are common constituents of soil and were not detected in the ground layer, their presence is likely attributable to contamination from the tomb environment, though the possibility of contribution from other unidentified inorganic additives cannot be entirely ruled out. In contrast, the ground layer (L2) exhibited manufacturing-related inorganic phases. Elemental signatures of sodium (Na), aluminum (Al), and silicon (Si) were detected at spot P1 in L2, thus

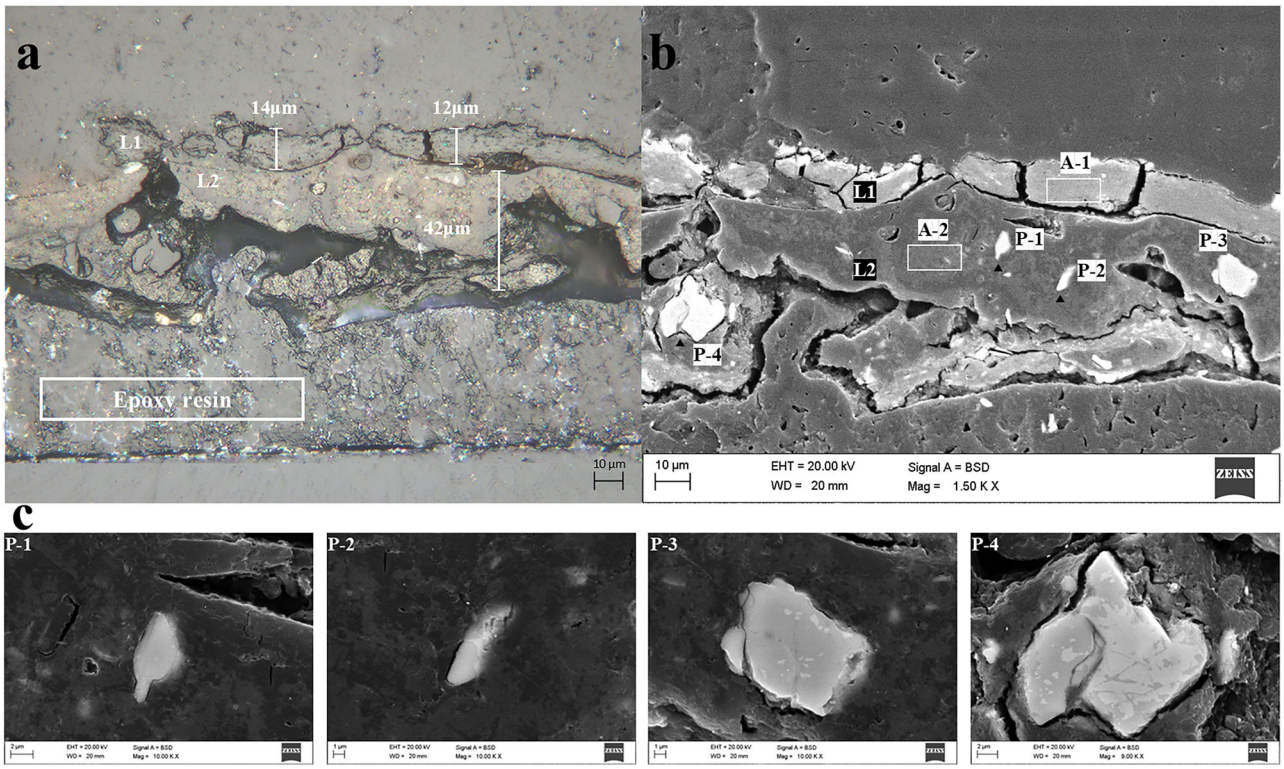


**Fig. 3 | The microscope photographs and BSE photograph of the lacquer film sample. a** The microscope photographs using bright field (BF) optical microscopy with halogen lamp illumination. **b** BSE photograph of the cross-section of the black lacquer sample. **c** BSE photographs of particles in L2.

**Table 1 | The composition of the points (areas) marked in Fig. 3b (wt%)**

| Marked area | C | O | K | Na | Al | Si | Ca | Fe |
|---|---|---|---|---|---|---|---|---|
| A-1 | 54.1 | 20.9 | – | – | – | 2.6 | 10.2 | 12.2 |
| A-2 | 79.8 | 14 | – | – | 1.5 | 3.3 | 1.4 | – |
| P-1 | 22.3 | 24.6 | – | 6.8 | 10.3 | 36 | – | – |
| P-2 | 29.1 | 29.3 | – | – | – | 41.6 | – | – |
| P-3 | 6.5 | 29.8 | | – | – | 63.7 | – | – |
| P-4 | 32.1 | 29.3 | – | – | – | 38.6 | – | – |

confirming the presence of sodium aluminosilicate compounds. Conversely, predominantly Si signals at spots P2-P4 definitively established the existence of silicon dioxide ($SiO_2$).

In order to further explore the composition of the material, micro-X-ray diffraction (μ-XRD) was utilized to continue the process of verification. The XRD pattern (Fig. 4) showed that the L2 layer was predominantly composed of quartz ($SiO_2$, JCPDS 00-078-1253), exhibiting characteristic Bragg peaks at 2θ 26.64°, 36.54°, 39.46°, 40.38°, 50.14°, 54.88°, 60.00°, 67.74°, 68.21°. In this study, sodium aluminum silicate ($NaAlSiO_4$, JCPDS 00-11-0221) was utilized at 2θ 20.93°, 27.48°, 35.08°, 42.58° in the ground layer with the objective of enhancing the physical or mechanical properties of lacquer film[16].

Historical records indicate that fillers for ground layers may include powdered pottery or porcelain, brick fragments, or natural clays[15]. These quartz-dominant mineral particles exhibit distinct characteristics based on the firing temperatures. Quartz, as a brittle mineral, fractures into angular particles. Its rapid $\alpha$-$\beta$ phase transitions occur at temperatures above 573 °C, generating discontinuous cracks within grains. Beyond 1000 °C, its melting produces rounded particles. Further heating develops prismatic or needle-like structures (tridymite or cristobalite)[17]. In the L2, quartz particles exhibited characteristic angular fractures (Fig. 3c), with no intra-crystalline cracks indicative of $\beta$-quartz phase transformation, confirming the absence of thermal processing. Sodium aluminum silicate particles feature a theoretical melting point of 1100 °C. These particles frequently coexist with quartz in ceramic filler systems, displaying smooth surface textures devoid of vitrified features or structural reorganization indicative of high-temperature exposure (Fig. 3c)[17]. The preservation of primary morphologies and intact crystal structures in both minerals confirms the use of uncalcined natural clay as the raw material.

Furthermore, the filler particles showed a narrow size distribution, with a range of 1~6 μm, which is significantly smaller than the natural fragmentation range of clay minerals, typically 10~100 μm[18]. This discrepancy indicates deliberate processing techniques, specifically crushing and graded sieving, consistent with historical records "sieving into coarse, medium, and fine grades" documenting the preparation method for the inorganic fillers in the ground layer[15].

### THM-Py-GC/MS analysis of the lacquer film

Secondly, in order to determine the type of lacquer used in the lacquer film, as well as other additives such as oils, the technique of THM-Py-GC/MS is also applied. The total ion chromatograms (TIC) of the lacquer film is depicted in Fig. 5, while the identified compounds are listed in Table 2. The identification of organic materials in the lacquer samples is based on AMDIS program developed by the National Institute of Standards and Technology (NIST) and RAdICAL excel developed by scientists at the Getty Conservation Institute and conservators at the J. Paul Getty Museum.

Lacquer sap is composed of polysaccharides, glycoproteins, laccase, water, and an abundant mixture of catechol substitutes in terms of chemical composition[19]. There are about 70 general and over 600 species of lacquer trees in the world, but only three main species of trees in the Anacardiaceae family have been found to produce lacquer, namely *Toxicodendron vernicifluum* (producing urushiol-based lacquer), primarily cultivated in China, Japan and Korea, *Toxicodendron succedaneum* (producing laccol-based lacquer), mainly grown in Taiwan and Vietnam, and *Gluta usitata* (producing thitsiol-based lacquer), mainly grown in Thailand, Laos, and

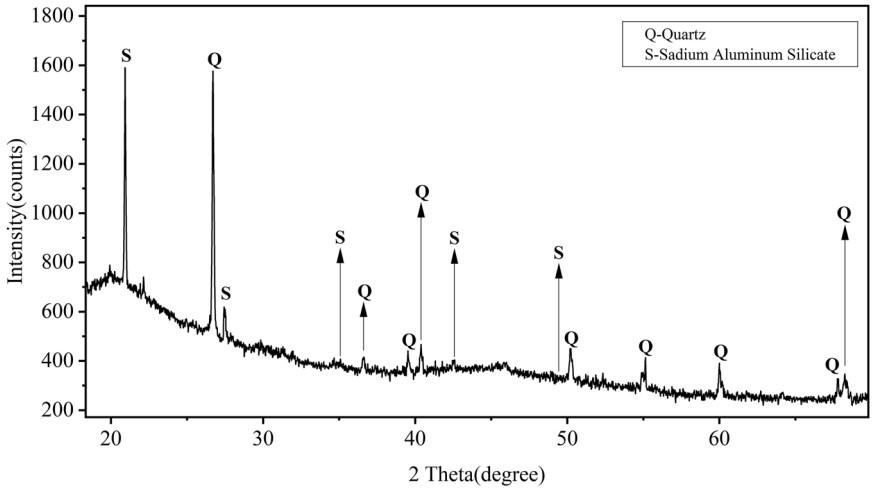


**Fig. 4 | The XRD pattern of the ground layers of the black lacquer layer.** X-ray diffraction pattern of the sample obtained from the black lacquer layer. Intensity (counts) is plotted as a function of diffraction angle (2θ degrees). The labeled peaks correspond to crystalline phases: Q for quartz ($SiO_2$) and S for sodium aluminosilicate.

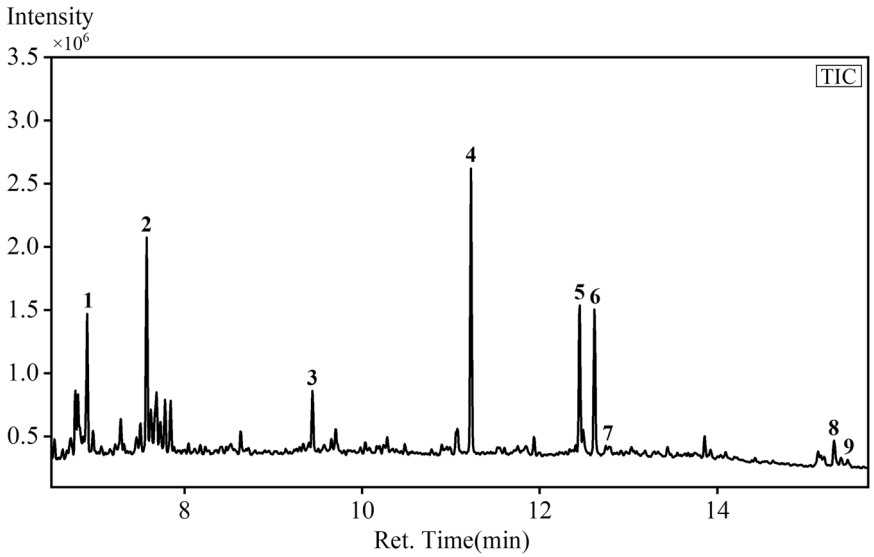


**Fig. 5 | The total ion chromatograms (TIC) of the black lacquer sample.** Total ion current (TIC) profile showing signal intensity versus retention time. Numbered peaks (1–9) indicate key organic compounds of the black lacquer sample detected.

**Table 2 | The list of main components of the black lacquer sample**

| Number | RT/ min | Peak area/% | Components identified |
|---|---|---|---|
| 1 | 6.9 | 2.71 | 1-Tetradecene |
| 2 | 7.58 | 3.57 | Naphthalene,decahydro-1,6-dimethyl-4-(1-methylethyl)- |
| 3 | 9.44 | 0.9 | Cadelene |
| 4 | 11.23 | 4.67 | Methyl hexadecanoate |
| 5 | 12.45 | 2.32 | Methyl oleate |
| 6 | 12.62 | 2.46 | Methyl stearate |
| 7 | 12.75 | 0.12 | Pyrene |
| 8 | 15.32 | 0.56 | 1, 2-Dimethoxy-3-pentadec-8-enylbenzene |
| 9 | 15.47 | 0.11 | Dimethylated 3-pentadecylcatechol |

Myanmar[20]. The actual distribution of lacquer trees is much wider. It is particularly evident in the *T. succedaneum* species which are also distributed in China, Malaysia, India, and Japan, apart from the above-mentioned places[21]. A recent study has revealed the use of laccol in a Neolithic-era lacquered pottery excavated from a site in Jiangsu Province, China. This finding suggests the potential for the growth of *T. succedaneum* in the lower reaches of the Yangtze River region during the Neolithic period[22]. The ageing process of lacquer generates alkanes, alkenes, and hydroxybenzenes and catechols. These compounds have been identified as the marker[4]. The markers of urushiol are mainly 3-pentadecylcatechol and its derivatives, and those of laccol are mainly 3-heptadecylcatechol and its derivatives. The markers of thitsiol are mainly 4-heptadecylcatechol and phenyl catechols[12,23–25], which can be used to indicate the presence or absence of lacquer and to trace the type and source of lacquer in ancient samples.

The Anacardiaceae compounds of the lacquer sample are displayed in Fig. 6, in which various homologous series of the marker compounds are presented and a recognizable visual form was created to distinguish the major Anacard types quickly and intuitively. The presence of dimethylated 3-pentadecylcatechol (C15) in the sample was detected. In addition, a series of alkanes, alkenes and alkyl benzenes were identified in the samples, with the highest content of heptane and pentadecane in alkanes, and that of 1-tetradecene in alkenes. Based on the analysis results, it can be concluded that urushiol-based lacquer from *Toxicodendron vernicifera* species was used in the lacquer film. Urushiol-based lacquer is the dominant lacquer identified in the lacquer objects from early China, as evidenced by the artifacts unearthed in the Geling tomb[4] and the Jiuliandun tomb[26] of the Chu

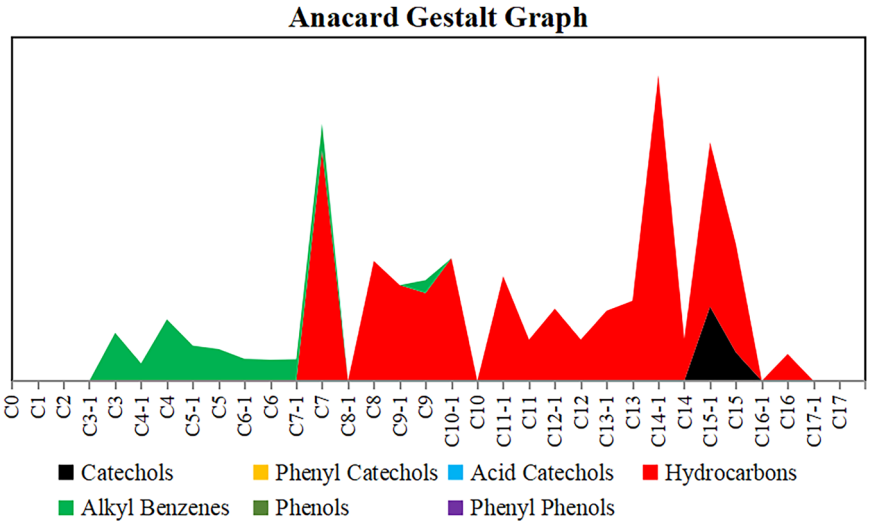


**Fig. 6 | The chemical composition of lacquer in the lacquer sample.** Anacard Gestalt profile showing the relative abundance of key phenolic homolog groups. X-axis: Homolog carbon-chain series. Y-axis: Relative quantity.

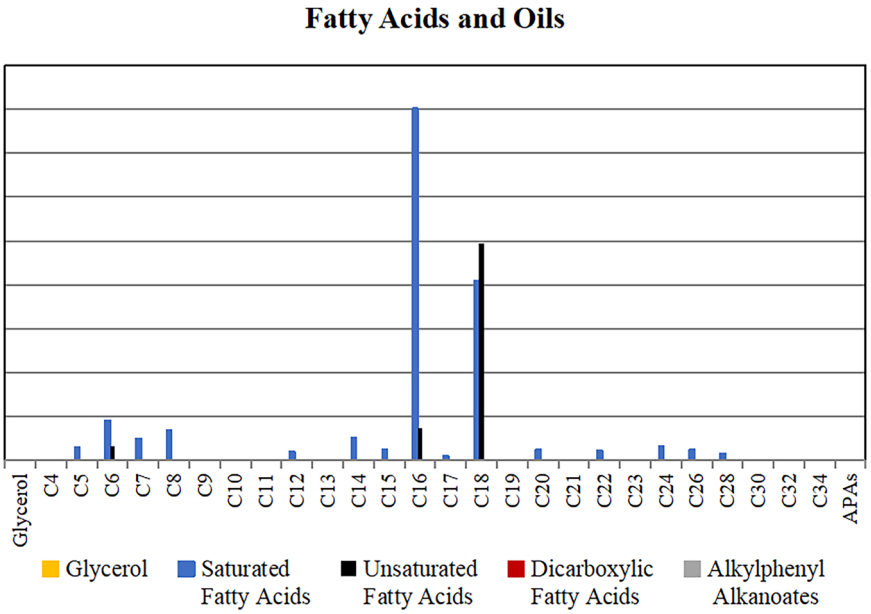


**Fig. 7 | The relative concentration of fatty acids in the lacquer sample.** Distribution of fatty acids components quantified by relative concentration.

state, and the Guojiamiao tomb of the Zeng state[27] during the Warring period states.

In addition, adalene and pyrene belonging to polycyclic aromatic hydrocarbons (PAHs) were identified in the lacquer sample. PAHs are volatile hydrocarbons of soot that are produced during the incomplete combustion of organic materials, such as coal, oil, wood, and tobacco. PHAs of soot were identified a phenanthrene, fluoranthene, pyrene, trisubstituted benzene, and benzo[k]fluoranthene and their isomers[28]. The detection of the pyrene and cadelene indicates the possible presence of soot in the sample, which is possibly used to color raw lacquer into black lacquer. Ancient Chinese records document that soot application in lacquering process served as a standard surface treatment[29]. The consistent detection of soot across multiple lacquer artifacts[4,10,30,31] confirms its prevalence as a conventional mineral pigment in lacquer.

There is no drying oil found in the lacquer film in the sample. Drying oils primarily consist of glycerol esters with minor free fatty acids. Oxidative degradation of unsaturated fatty acids generates characteristic dicarboxylic acids including suberic acid, azelaic acid, and sebacic acid, among which azelaic acid predominates[11]. Consequently, glycerol and azelaic acid serve as diagnostic markers for identifying drying oils in cultural materials[4]. Figure 7 shows the relative concentration of fatty acids present in the lacquer sample. It revealed the absence of glycerol (yellow bar in Fig. 7) and dicarboxylic fatty acids, especially azelaic acid (red bar in Fig. 7), indicating no drying oil used in the lacquer film of Madao. The lacquer samples of chariots from Geling tomb showed abundant fatty acid components, with azelaic acid detected within the mixture[4]. Similar oil traces occurred in ear cups and boxes from Jiuliandun tomb[1] and the lacquer scabbard from Lijiaba site[32]. These examples show that the addition of drying oils to lacquer films during the Warring States period was most commonly used but not fully standardized practice.

### Py-GC/MS analysis of the fibers

Two analytical methods were employed to characterize the fibers used in the Madao artifact.

Firstly, results of the Py-GC/MS analysis of the fibers are presented below. Figure 8 depicts the specifics of the micrograph of the fiber sample in the M1:N44 Madao (Fig. 2d, e). There were two types of fibers (yellow and black) used, exhibiting a noticeable contrast in appearance. The black fibers


**Fig. 8 | The schematic detail of the M1: N44 Madao fiber sample. a** The original morphology of the fiber sample (white circle) demonstrates the characteristic that yellow fibers enveloping black fibers. OM X150: Optical microscopy of 150X magnification. **b** Sampling locations for Py-GC/MS analysis. Area 1 (white rectangle 1) for yellow fiber sampling. Area 2 (white rectangle 2) for black fiber sampling. OM X200: Optical microscopy of 200X magnification.

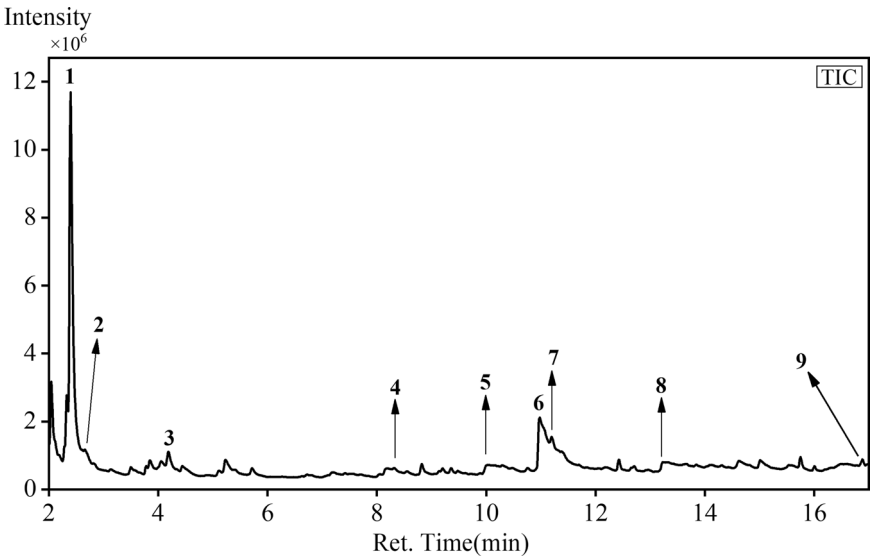


**Fig. 9 | The total ion chromatograms (TIC) of the yellow fiber sample.** Total ion current (TIC) profile showing signal intensity versus retention time. Numbered peaks (1–9) indicate key organic compounds of the yellow fiber sample detected.

were enveloped within the yellow one (Fig. 8a). To identify the types of the two fibers, appropriate samples were taken and analyzed by Py-GC/MS. Area 1 was the yellow fiber sampling location. Area 2 was the black fiber sampling location.

The TIC of yellow fibers are depicted in Fig. 9, while the identified compounds are listed in Table 3. Cellulose is the primary structural component of plant cell walls and is often associated with hemicellulose and lignin. Cellulose is formed from D-glucopyranose units linked by *β*-O-4 glycosidic bonds[33]. The main pyrolysis products of cellulose were pyranoids, furans, aldehydes, ketones, and linear small molecules[34]. Lignin is a three-dimensional, complex biopolymer comprised of phenylpropanoid units, specifically syringyl (S), guaiacyl (G), and *p*-hydroxyphenol (H) monomers, linked via dehydrogenation reactions[35]. During the pyrolysis of lignin, compounds such as phenol, toluene, benzaldehyde, and benzyl alcohol are generated[36]. The 2-furanmethanol, 3-Butene-1,2-diol, 1-(2-furanyl)-2-methyl- and 3,6-Octadienal, 3,7-dimethyl detected in the yellow fiber sample were derived from cellulose. And the presence of benzene derivatives, including toluene, benzaldehyde, phenol and benzyl alcohol, were derived from lignin. Therefore, the composition of yellow fibers is more closely aligned with that of plants.

The TIC of black fibers are depicted in Fig. 10, while the identified compounds are listed in Table 4. Cholesterol is a crucial component of animal cell membranes and can be converted into unsaturated steroidal compounds through enzymatic reactions during metabolic process[37]. Animal derivation of the black fiber sample is demonstrated through detection of 2-cholestene, which constitutes a cholesterol derivative absent in botanical sources. Feathers are complex structures composed of keratin, collagen, pigments, lipids, and water. Among them, keratin is the most important component that gives feathers good elasticity and softness. Glycine, serine, proline, threonine, threonine, valine and lysine are the basic building blocks of keratin[38]. The pyrrole and its derivatives detected in the black fiber sample were derived from collagen. Cyclo[D-Leu-L-Pro-], Cyclo(Gly-Pro-) and their derivatives detected in the samples were derived from proline belonging to keratin in feathers[39]. Therefore, there is compelling evidence supporting the identification of the black fiber samples as animal fibers, with chemical composition analysis further revealing characteristics consistent with animal feathers.

**Table 3 | The list of main components of the yellow fiber sample**

| Number | RT/min | Peak area/% | Chemical substance |
|---|---|---|---|
| 1 | 2.4 | 66.3 | Toluene |
| 2 | 2.66 | 0.58 | 2-Furanmethanol |
| 3 | 4.19 | 3.96 | Ethylbenzene |
| 4 | 8.32 | 0.31 | Benzaldehyde |
| 5 | 10.03 | 3.04 | Phenol |
| 6 | 10.98 | 18.04 | Benzyl alcohol |
| 7 | 11.2 | 3.61 | 3,6-Octadienal, 3,7-dimethyl- |
| 8 | 13.23 | 3.47 | *p*-Cresol |
| 9 | 16.88 | 0.7 | 3-Butene-1,2-diol, 1-(2-furanyl)-2-methyl- |

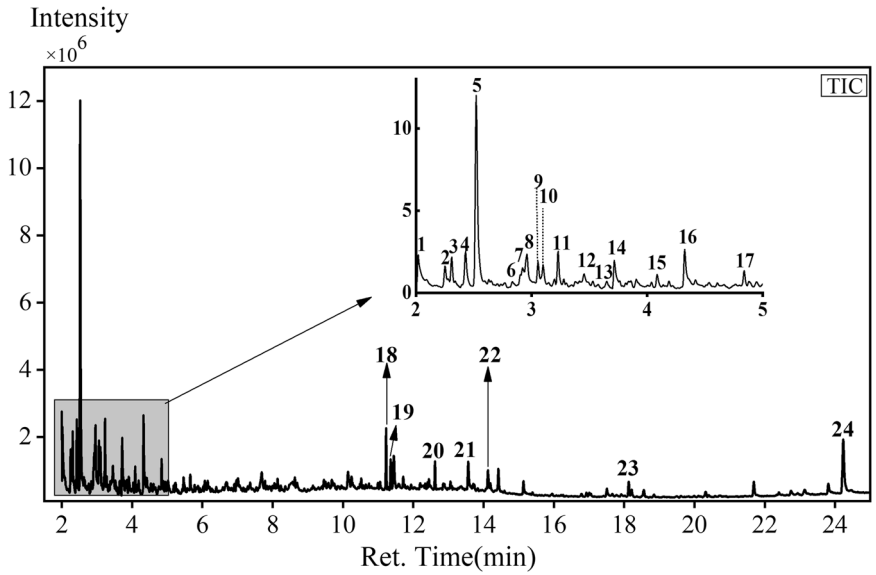


**Fig. 10 | The total ion chromatograms (TIC) of the black fiber sample.** Total ion current (TIC) profile showing signal intensity versus retention time. Numbered peaks (1–24) indicate key organic compounds of the black fiber sample detected.

**Table 4 | The list of main components of the black fiber sample**

| Number | RT/min | Peak area/% | Chemical substance |
|---|---|---|---|
| 1 | 2.02 | 3.51 | 1-Ethenylaziridine |
| 2 | 2.25 | 2.62 | Trans-2-Hexene |
| 3 | 2.31 | 4.16 | 3-Methylbutanenitrile |
| 4 | 2.43 | 5.52 | Pyrrole |
| 5 | 2.52 | 25.68 | Toluene |
| 6 | 2.83 | 1.08 | 2-Methylpyridine |
| 7 | 2.92 | 4.19 | 2-Methyl-1H-pyrrole |
| 8 | 2.96 | 5.98 | 3-Methyl-1H-pyrrole |
| 9 | 3.06 | 3.8 | Ethylbenzene |
| 10 | 3.1 | 3.36 | 1,3-Dimethylbenzene |
| 11 | 3.23 | 4.03 | Styrene |
| 12 | 3.38 | 2.52 | 2,5-Dimethyl-1H-pyrrole |
| 13 | 3.65 | 0.95 | Benzaldehyde |
| 14 | 3.72 | 4.2 | Phenol |
| 15 | 4.09 | 1.57 | Benzyl alcohol |
| 16 | 4.33 | 5.75 | 4-Methylphenol |
| 17 | 4.84 | 1.63 | Benzyl cyanide |
| 18 | 11.23 | 3.34 | Methyl hexadecanoate |
| 19 | 11.35 | 2.06 | Cyclo[D-Leu-L-Pro-] |
| 20 | 12.62 | 1.58 | Methyl stearate |
| 21 | 13.57 | 2.57 | 2,3,6,7,8,8a-Hexahydro-1,4-dioxopyrrolo[1,2-a]pyrazine-3-propanamide |
| 22 | 14.13 | 1.44 | Cyclo(Gly-Pro) |
| 23 | 18.13 | 1.21 | Cholest-2-ene |
| 24 | 24.23 | 7.24 | m,m-Quaterphenyl |

### Polarized light micro analysis of the fibers

Secondly, based on the Py-GC/MS analysis, the yellow fibers were identified as plant fibers, while the black fibers were determined to be animal feather fibers. To further identify the specific species, polarized light microanalysis of the fibers was performed on the two types of samples after staining treatment with Herzberg reagent.

As illustrated in Fig. 11a, b, the yellow fiber width shows a non-uniform distribution, with some portions of the same fiber displaying a width greater than the average (~20 μm), while other portions exhibit a narrower width. In addition, the fibroblast cavities of the samples were obvious, but the diameters showed inconsistency, and the smaller fibroblasts were linearly arranged or even disappeared. All of the above features are more consistent with bast fibers[40], indicating that the yellow fibers in the sample were identified as bast fibers (see Supplementary Note 1). Archaeobotanical evidence attests to over 5000 years of bast fiber usage in China[41]. Historical texts from the Warring States period, such as the *Zuozhuan* (左传), contained numerous accounts of bast fiber usage, establishing it as one of predominant textile material of this era[42]. Bast fibers demonstrate superior tassel-binding capabilities through their naturally elongated morphology, resilient mechanical behavior, and effective moisture regulation capacity, fulfilling the functional requirements for securing ceremonial ornaments[43]. These material traits explained the use of bast fibers in Madao artifacts.

Figure 11c, d presents micrographs of black fibers stained with Herzberg reagent, revealing naturally crimped patterns characterized by rounded nodal structures and elliptical pigment aggregations. Width measurements on Fig. 11d confirms these fibers exhibit internodal lengths of 10~20 μm, node diameters of 5~6 μm, and barbule diameters of 3~5 μm (detailed in Supplementary Note 1). These morphological characteristics correspond to the down feather ultrastructure of *Hydrophasianus chirurgus*[44].

*H. chirurgus* is also called the pheasant-tailed Jacana, and it belongs to the *Jacanidae* species, which is a historically common migratory bird and now a national Class II protected animal in southern China. It possesses elongated tail feathers that were considered suitable for decorative tassels in ancient China. Yong Cai of the Eastern Han Dynasty wrote that Madao was made of tail feathers of yak[45]. Shao Ying, a contemporary of Yong Cai, had a different view. He believed that the tassel was made of tail feathers of "Zhi" (雉)[46]. In ancient China, "Zhi" generally referred to the pheasant[47]. The morphological and naming similarities between pheasant and pheasant-tailed Jacana suggest the pheasant-tailed Jacana may have been included in the "Zhi" category within contexts like Madao ornamentation. Although modern comparative studies are hindered by the species' current status as a Class II protected animal in China[48], the combined evidence of morphological consistency, historical accessibility, and functional suitability supports the identification of the black fibers as down feathers from *H. chirurgus*.

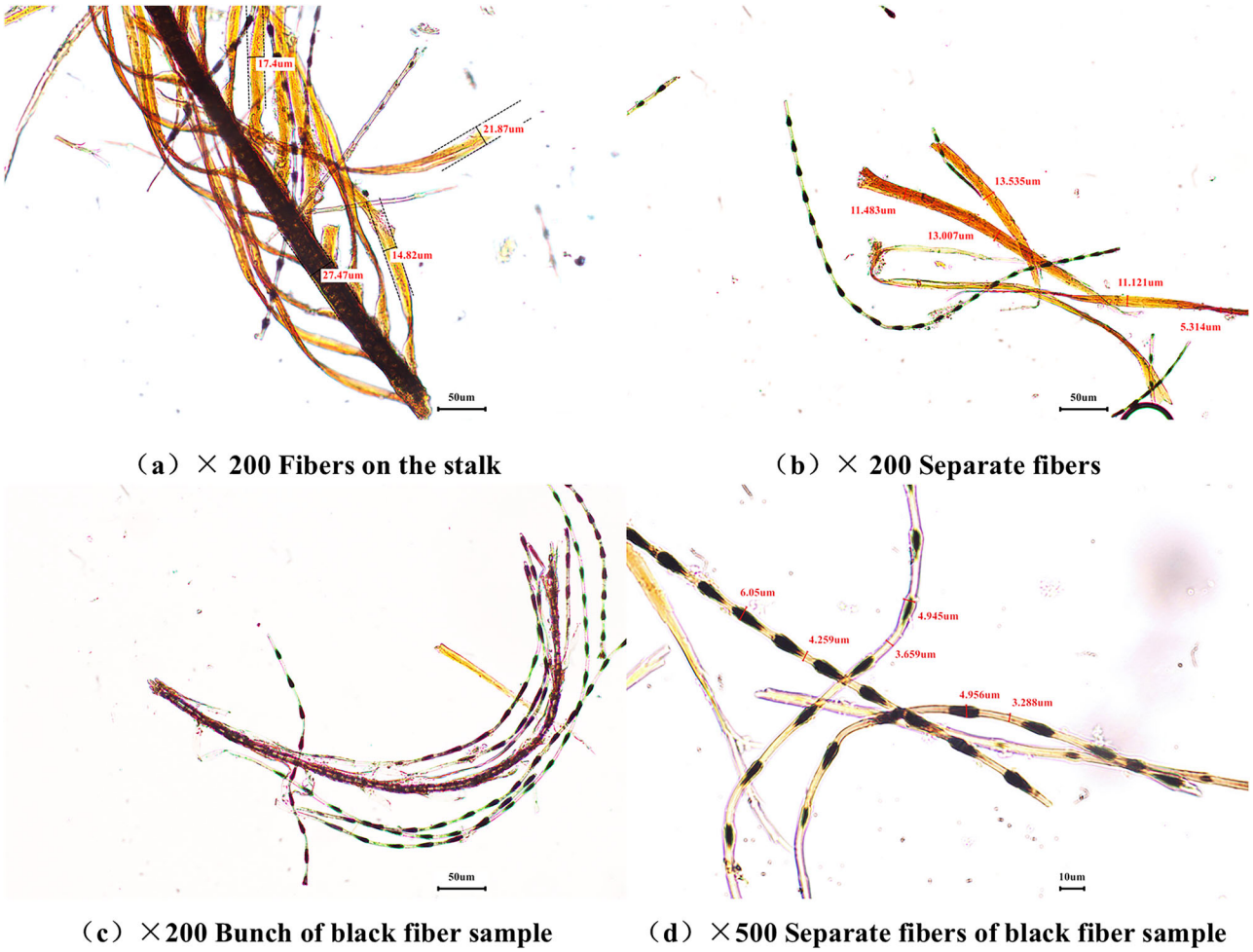


**Fig. 11 | Yellow and black fibers after staining with Herzberg's reagent. a** Yellow fiber bundle on stalk (×200) with width measurements. **b** Separated yellow fibers (×200) with width measurements. **c** Bunch of black fiber sample (×200). **d** Separated fibers of the black fiber sample (×500) with width measurements.

## Discussion

The Madao artifacts from Wangshanqiao M1 in the middle Warring States Period were analyzed by multi-techniques. Their wooden bases were painted with a two-layer structure, including the lacquer layer and the ground layer. Within the ground layer, size-sorted clay particles served as inorganic fillers. Microscopic analysis confirmed their unheated state, identifying them as natural clay. These bases were coated with urushiol-based lacquer devoid of drying oils. The tassels were made of the feathers of *H. chirurgus*, which was held in place with bast fibers. Collectively, these findings comprehensively elucidate Madao techniques and materials, providing robust scientific evidence for chariot and horse components production during the Warring States period.

This study represents the first scientific characterization of the Madao artifact, providing a significant case study on the craftsmanship of composite lacquerwares. The artifact incorporated multiple materials, including urushiol-based lacquer, feathers of *H. chirurgus*, and bast fibers. Unlike laccol-based and thitsiol-based lacquer, urushiol-based lacquer contains less moisture, thereby offering superior material properties. The Hubei region has a warm and humid climate, which supports the widespread distribution of *Toxicodendron vernicifera* and bast fibers. Furthermore, it is a suitable habitat for species such as *H. chirurgus*. Therefore, the above three materials were readily available locally. Natural clay, being widely available, was less likely to have been transported over long distances. It is therefore highly probable that the artifact was manufactured using mainly local materials. Technologically, the Madao differs from other lacquer objects such as ear cups and boxes, adding new insights into the lacquer production system of the Chu culture. While it is important to note that due to the limited sample quantity, this study may not fully represent all craft features of this type of artifact. Nonetheless, these finding offer valuable insights into the diversity and complexity of lacquer production in ancient China.

Received: 12 June 2025; Accepted: 25 September 2025;
Published online: 07 October 2025

## References

1. Fu, Y., Chen, Z., Zhou, S. & Wei, S. Comparative study of the materials and lacquering techniques of the lacquer objects from Warring States Period China. *J. Archaeol. Sci.* **114**, 105060 (2020).
2. Ni, L. Research on lacquer ware from the WuWangDun tomb in Huainan. *J. Fuyang Normal Univ. Soc. Sci. Editor.* **1**, 1–7 (2025).
3. Wang, X. et al. Excavation report of M1 at Jiuliandun Site of Zaoyang, Hubei province. *Jianghan Archaeol.* **145**, 20–70 (2019).
4. Wei, S. et al. Analytical characterization of lacquer objects excavated from a Chu tomb in China. *J. Archaeol. Sci.* **38**, 2667–2674 (2011).
5. Fu, Y., Wei, S., Yang, J. & Guan, L. Research on the films of ancient lacquerwares by thermally assisted hydrolysis-methylation (THM) pyrolysis-gas chromatography/mass spectrometry (Py-GC/MS) analysis. *Sci. Conserv. Archaeol.* **30**, 53–59 (2018).
6. Pang, Z. Madao in the Warring States, Qin and Han Dynasties and related issues. *Archaeology* **11**, 101–111 (2019).
7. Zhang, D. & Jing, L. Madao, or Mamao?. *J. Liaoning Normal Univ.* **46**, 126–132 (2023).

8. Jia, H. et al. Briefing on the excavation of No.1 Chu Tomb at Wangshanqiao, Jingzhou, Hubei, China. *Chin. Cult. Relics.* **2**, 4–37 (2017).
9. He, Q. The application of scientific and technological analysis in the study of ancient lacquerware production process. *A Collection of Essays about Capital Museum of China*. **0**, 351–356 (2012).
10. Zhu, Z. et al. Shedding new light on lacquering crafts from the Northern Wei Dynasty (386–534 CE) by revisiting the lacquer screen from Sima Jinlong's Tomb. *J. Cult. Herit.* **71**, 309–319 (2025).
11. Schilling, M. R., Heginbotham, A., van Keulen, H. & Szelewski, M. Beyond the basics: asystematic approach for comprehensive analysis of organic materials inAsian lacquers. *Stud. Conserv.* **61**, 3–27 (2016).
12. Qin, Y. et al. Exploring thitsi in Qing Dynasty lacquerware: Insights from a preliminary study. *npj Herit. Sci.* **13**, 46 (2025).
13. Nacci, T. et al. Characterization of textile fibers by means of EGA-MS and Py-GC/MS. *J. Anal. Appl. Pyrolysis* **165**, 105570 (2022).
14. Lian, Q., Qiu, S., Shi, D. & Pei, D. Identification of three elastic fibers by thermal cracking gas chromatography-mass spectrometry. *Synth. Fiber China* **46**, 48–53 (2017).
15. Huang, C.& Yang, M. Xiushi lu. *J. Chin. Lacq.* **10**, 43–48 (1991).
16. Jin, P., Hu, Y. & Ke, Z. Characterization of lacquer films from the middle and late Chinese warring states period 476–221BC. *Microsc. Res. Tech.* **80**, 1344–1350 (2017).
17. Eramo, G. Ceramic technology: how to recognize clay processing. *Archaeol. Anthropol. Sci.* **12**, 164 (2020).
18. Montana, G. Ceramic raw materials: how to recognize them and locate the supply basins-mineralogy, petrography. *Archaeol. Anthropol. Sci.* **12**, 175 (2020).
19. Körber, U., Schilling, M. R., Dias, C. B. & Dias, L. Simplified Chinese lacquer techniques and *Nanban* style decoration on Luso-Asian objects from the late sixteenth or early seventeenth centuries. *Stud. Conserv.* **61**, 68–84 (2016).
20. Yin, L. et al. Bacterial and biodeterioration analysis of the waterlogged wooden lacquer plates from the Nanhai No. 1 Shipwreck. *Appl. Sci.* **9**, 13 (2019).
21. Hiraoka, Y., Tamaki, I. & Watanabe, A. The origin of wild populations of *Toxicodendron succedaneum* on mainland Japan revealed by genetic variation in chloroplast and nuclear DNA. *J. Plant Res.* **131**, 225–238 (2018).
22. Shi, S. et al. Identification of laccol as a paint binder in Neolithic pottery from China. *J. Archaeol. Sci.* **173**, 106–119 (2025).
23. Ma, X. et al. Characterization of early imperial lacquerware from the Luozhuang Han Tomb China. *Archaeometry* **59**, 121–132 (2017).
24. Niimura, N., Miyakoshi, T., Onodera, J. & Higuchi, T. Characterization of Rhus vernicifera and Rhus succedanea lacquer films and their pyrolysis mechanisms studied using two-stage pyrolysis-gas chromatography/mass spectrometry. *J. Anal. Appl. Pyrolysis* **37**, 199–209 (1996).
25. Vogl, O. Oriental lacquer, poison ivy, and drying oils. *J. Polym. Sci. Pol. Chem.* **38**, 4327–4335 (2000).
26. Fu, Y., Xiao, Q., Zong, S. & Wei, S. Characterization and quantitation study of ancient lacquer objects by NIR spectroscopy and THM-Py-GC/MS. *J. Cult. Herit.* **46**, 95–101 (2020).
27. Chen, Z., Wei, S., Fu, Y. & Fang, Q. Analysis of lacquer from the Zeng Cemetery (1046-771 BCE) at Guojiamiao. *Coatings.* **14**, 1559 (2024).
28. Wei, S. et al. Identification of the materials used in an Eastern Jin Chinese ink stick. *J. Cult. Herit.* **13**, 448–452 (2012).
29. Han, F. *Han Fei Zi* (Zhonghua Book Company, 2015).
30. Fu, Y. *Study on Lacquerring Materials and Techniques in the Eastern Zhou, Qin and Han Dynasties*. Doctoral dissertation (University of Science and Technology Beijing, 2023).
31. Garner, H. Technical studies of oriental lacquer. *Stud. Conserv.* **8**, 84–98 (1963).
32. Han, B. et al. The lacquer crafting of Ba state: Insights from a Warring States lacquer scabbard excavated from Lijiaba site (Chongqing, southwest China). *J. Archaeol. Sci. Rep.* **42**, 103416 (2022).
33. Etale, A., Onyianta, A. J., Turner, S. R. & Eichhorn, S. J. Cellulose: a review of water interactions, applications in composites, and water treatment. *Chem. Rev.* **123**, 2016–2048 (2023).
34. Wang, S. et al. Mechanism research on cellulose pyrolysis by Py-GC/MS and subsequent density functional theory studies. *Bioresour. Technol.* **104**, 722–728 (2012).
35. Lupoi, J. S. et al. Recent innovations in analytical methods for the qualitative and quantitative assessment of lignin. *Renew. Sust. Energy Rev.* **49**, 871–906 (2015).
36. Chen, W. et al. Cellulose pyrolysis under $NH_3$ atmosphere for levoglucosan and pyrrole: an experimental and theoretical study. *Fuel* **361**, 130686 (2024).
37. Zhang, L., Shi, Y., Liang, B. & Li, X. An overview of the cholesterol metabolism and its proinflammatory role in the development of MASLD. *Hepatol. Commun* **8**, e0434 (2024).
38. Ling, S. Extraction of edible protein from feathers by hydrolysis. *Prac. Rural Sci. Technol. Inf.* **4**, 19 (1996).
39. Wang, N. et al. Identification of protein binding media used in Chinese cultural relics by pyrolysis-gas chromatography/mass spectrometry. *Chin. J. Anal. Chem.* **48**, 90–96 (2020).
40. Yi, X. *Microscopic Atlas of Plant Fibers of Ancient and Traditional Chinese Handmade Paper* (Guangxi Normal University Press Co. Ltd, 2022).
41. CPAM Chekiang Province, Chekiang Provincial Museum. Excavations (first season) at HO-MU-TU in YU-YAO county, Chekiang province. *Acta Archaeol. Sinica.* **1**, 39–94 (1978). 140-155.
42. Zuo, Q. *Chun Qiu Zuo Zhuan Zhu* (Zhonghua Book Company, 1981).
43. Jiang, W. et al. Monitoring chemical changes on the surface of kenaf fiber during degumming process using infrared microspectroscopy. *Sci. Rep.* **7**, 1240 (2017).
44. Brom, T. G. Microscopic identification of feathers and feather fragments of Palearctic birds. *Bijdragen tot de dierkunde* **56**, 181–204 (1986).
45. Cai, Y. *Du Duan* (Zhonghua Book Company, 1985).
46. Guan, X. *Er Ya*. (Zhonghua Book Company, 2016).
47. Lu, T. & He, P. The pheasant in classical Chinese literature. *For. Humankind.* **3**, 98–101 (2014).
48. Wang, Z. Order No. 7 of the state forestry administration - directory of terrestrial wildlife that is protected by the state for its beneficial or significant economic and scientific research value. *Chin. J. Wildl*. **5**, 49−82 (2000).


## Acknowledgements

Authors would like to acknowledge the financial support from the National Social Science Fund (23CKG025). We would also thank Michael R. Schilling in Getty Conservation Institute for the technological support of RAdICAL system.

## Author contributions

L.L. completed the experiments, data analysis and draft of the article. Y.F. performed data analysis, experimental design, and manuscript drafting. Y.Z. revised the experimental details. J.L. involved in archaeological excavation and provided the sample information. S.W. provided the guidance on experiments and conceived the outline of the paper. All authors participated in the discussion and conclusion of the paper.

## Competing interests

The authors declare no competing interests.

## Additional information

**Supplementary information** The online version contains supplementary material available at https://doi.org/10.1038/s40494-025-02080-4.

**Correspondence** and requests for materials should be addressed to Yingchun Fu or Shuya Wei.